BUTTERWORTH HEINEMANN

Polymer Vol. 36 No. 4, pp. 731–742, 1995

0032-3861/95/$10.00+0.00

In situ observation of the plastic deformation of polypropylene spherulites under uniaxial tension and simple shear in the scanning electron microscope

M. Aboulfaraj*, C. G'Sell, B. Ulrich and A. Dahoun
Laboratoire de Métallurgie Physique et Science des Matériaux, URA CNRS No. 155, Ecole des Mines, Parc de Saurupt, 54042 Nancy, France
(Received 6 September 1993; revised 25 April 1994)

The α- and β-spherulites in polypropylene (PP) were identified by direct observation in the scanning electron microscope after appropriate etching. The α-phase has a dark contrast while the β-phase is brighter. Results concerning the individual behaviour of α- and β-spherulites in polypropylene samples which have been subjected to tensile and shear loading are reported. Under tensile loading, the α-spherulites exhibit a brittle behaviour, while the β-phase deforms plastically up to high deformations. The brittle behaviour of the monoclinic structure is characterized by cavitation at an early stage of deformation at the spherulites boundaries or at their equatorial region perpendicular to the tensile axis. Under shear loading, the α-phase cavitation disappears and both phases are then capable of undergoing large strains. However, quantitative characterization of the local deformation in each spherulite species showed that the α-structure deforms less than the global deformation while the β-phase compensates for this lack of plastic deformation of the other phase. The interlocked structure of the α-spherulites is discussed as being the leading contributing factor towards their brittleness, since it makes the plastic glide of this phase very difficult. In contrast, the radial lamellae of the β-spherulites allow the initiation and propagation of plastic glide more easily. The presence of a β-phase in PP with coarse spherulites considerably improves the mechanical properties at room temperature.

(Keywords: polypropylene; spherulites; plastic deformation)

INTRODUCTION

The crystalline structure of isotactic polypropylene (PP), is one of the most complex among industrially developed polymeric materials, since it displays several allotropic modifications and a variety of spherulitic morphologies. The two most common crystalline phases, which were extensively studied by Natta *et al.*[1] and other workers[2–4], contain monoclinic (α-) and hexagonal (β-) unit cells, respectively. It was shown that both crystalline structures can coexist in a given specimen, but with each spherulite consisting of a single phase. The α-species are characterized by the presence of transversal (or 'daughter') crystallites, in addition to the principal framework of radial lamellae. As for the β-spherulites, they display radial lamellae only, but with two alternative variants, namely straight lamellae with a sheaf-like structure in one case, and curved lamellae in the other case[3,4].

Considering this structural complexity, it is conceivable that the mechanical behaviour of a given PP sample should be highly dependent on its processing history, through the relative proportions of the different phases and/or spherulite morphologies. In particular, the plastic response (yield stress, consolidation, failure mechanisms) should be extremely variable on the spherulitic scale, as well as at the macroscopic level.

Studying the mechanical behaviour of PP at the microstructural level necessitates characterization of the deformation and/or crazing mechanisms within individual spherulites of an identified crystalline structure. Although transmission electron microscopy (TEM) provides the highest resolution for such observations, it requires the microtoming of thin films from the bulk samples after unloading, with serious risks of relaxation and degradation. In contrast, scanning electron microscopy (SEM) allows direct and dynamic observation of the spherulites during the course of a mechanical test with bulk specimens, providing that special techniques are used in order to reveal the microstructute and to apply the deformation *in situ* directly within the microscope stage.

Following a recent study[5] in which the present authors showed that the fine morphologies of the α- and β-spherulites could be differentiated using SEM observations after adequate etching of the PP with an acidic mixture, the aim of this paper is to investigate the deformation modes of the two phases under uniaxial tension and simple shear in bulk samples stressed by means of a miniaturized testing machine which has been especially developed for this work. After the main experimental results are presented, they will be

*To whom correspondence should be addressed

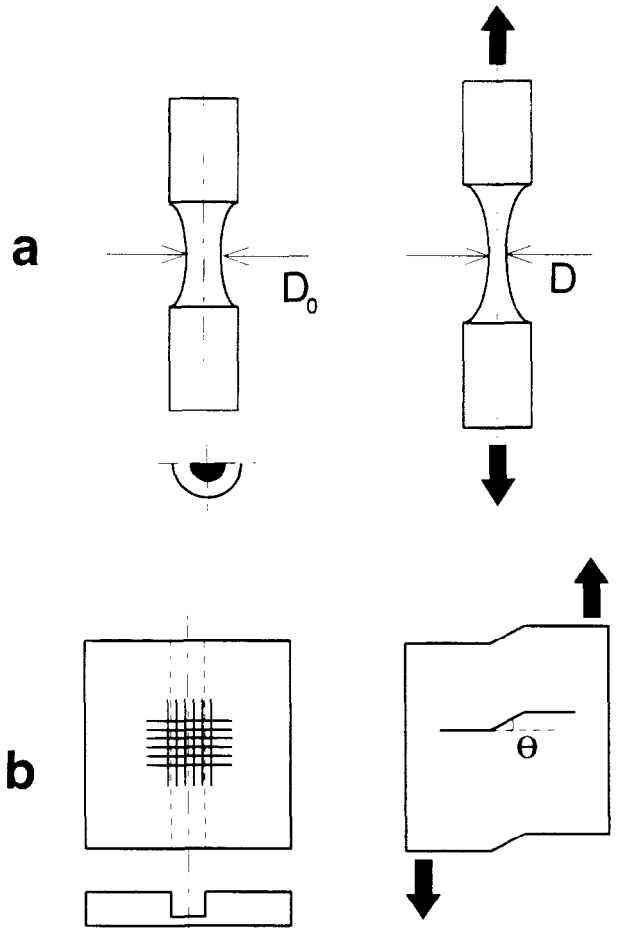

Figure 1 Geometry of the polypropylene samples used for the uniaxial tension and simple shear tests performed in the scanning electron microscope

interpreted in terms of the microstructural features of the two crystalline modifications.

MATERIAL AND METHODS

Specimen preparation

The polypropylene used in this work was manufactured by Atochem (3050 MN1), and is characterized by a relatively broad molecular weight distribution, as assessed by gel permeation chromatography, with $\overline{M}_w = 75\,940\ g\ mol^{-1}$ and $\overline{M}_n = 26\,220\ g\ mol^{-1}$. The polymer was processed in a thick mould (300 × 200 × 15 mm) designed for producing parallelepipedic plates. The process consists of extruding the melt slowly in the mould and then continuing to feed the mould under the extruding pressure during the cooling sequence. The plates thus obtained have negligible orientation, and possess much less chain degradation and contain less bubbles than observed for samples obtained from conventional injection or extrusion techniques. In addition, the cooling rate is relatively slow and the semicrystalline structure is quite reproducible.

Special samples were carefully machined from the extruded plates, according to the mechanical test applied. In the case of the uniaxial tension tests, specimens were utilized whose shape is directly deduced from the hourglass type recommended in a previous paper[6]. This shape was preferred to standard samples with a constant cross-section, since it induces the onset of necking in a predefined zone, which makes easier the correlation of the first plasticity events at a microscopic scale as the deformation proceeds at the overall level. However, since the SEM technique restricts observations to the surface only, it was decided to truncate the originally axisymmetric specimens along a plane containing the tensile axis (*Figure 1a*). We will assume here, to a first approximation, that the mechanisms observed in this plane are similar to those occurring along the axis within an unsplit sample. In the case of the simple shear tests, the specimens have identical proportions (providing a 0.5 homothetical reduction) to those used several times previously for the determination of the plastic behaviour of thermoplastics or thermosets[7,8]. They have a parallelepipedic shape with a longitudinal notch which is 5 mm deep and 4 mm wide (*Figure 1b*). Similar to the case of the tension studies, this geometry favours the localization of the plastic deformation within the predefined plane at the root of the notch where the attention is focused while the test is being run.

For both types of specimens, the flat surface was polished with several diferent emery papers, and finally with a very fine alumina powder (0.05 mm) until no residual scratches were visible. They were subsequently immersed for 18 h in the solution recommended by Olley and Basset[9-11] for observation of the spherulitic structure of PP, i.e. 1.3 wt% potassium permanganate, 32.9 wt% concentrated H_3PO_4 and 65.8 wt% concentrated H_2SO_4. They were rinsed several times with distilled water, hydrogen peroxide and then finally with acetone, in order to avoid any artefacts caused by pollution effects and subsequently sputtered with a very thin layer of gold. The above operations result in the amorphous part of the spherulites being etched preferentially, and thus we can reveal their substructure through direct observations with a standard JEOL SEM 820 microscope operating in the secondary electron mode. The optimum resolution/charge effects ratio was obtained with an accelerated electron voltage in the range from 2 to 6 kV. As discussed in detail in a previous paper[5], the crystalline structures of individual spherulites are easily differentiated in samples prepared according to the above method since the β-spherulite appear with a bright contrast while the α-species exhibit a dark aspect (*Figure 2*).

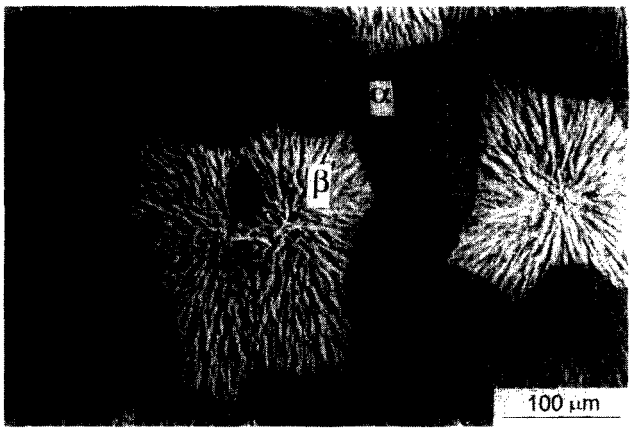

Figure 2 Morphology of the α- and β-spherulites revealed in a sample of polypropylene after polishing and chemical etching (the α-phase is the dark one)

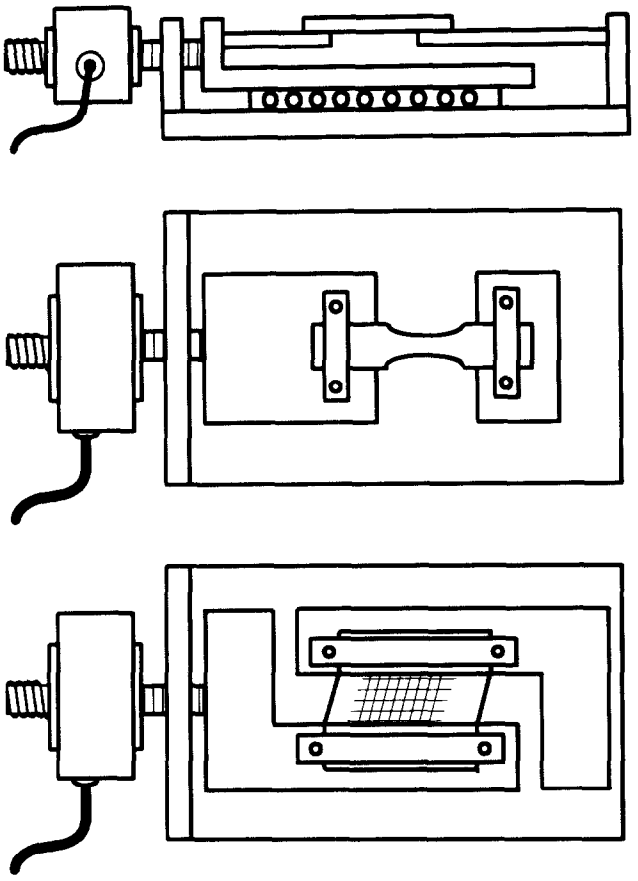

Figure 3 Schematic diagram of the deformation apparatus

In situ *mechanical testing techniques*

In order to carry out these tests, a special apparatus was developed in our laboratory. This is composed of a miniaturized testing machine which fits inside the scanning electron microscope chamber, and a control unit which is located on the microscope board. The machine is based on a translation device (*Figure 3*), equipped with low-friction linear ball bearings (Schneeberger) and driven by a high-torque, d.c.-voltage motor which allows speeds of between 0.25×10^{-4} and 1.75×10^{-2} mm s^{-1}. Two alternative sets of grips are available, which have been especially designed for tension and shear tests, respectively, with a maximum loading capacity of ~ 200 N.

In the uniaxial tensile tests, the deformation is investigated in the weakest cross-section of the samples. In a previous paper from our laboratory[12], it was shown that the tensile strain in this cross-section is nearly homogeneous at the macroscopic level, due to reasons of symmetry. In the case of plastically deforming materials under isochoric conditions, the effective strain ε is directly obtained from the reduction in diameter through the following relationship:

$$\varepsilon = \varepsilon_{zz} = 2\varepsilon_{rr} = 2 \ln (D_0/D) \quad (1)$$

where ε_{zz} and ε_{rr} measure the axial and radial strains, respectively, in the plane with the minimum cross-section whose diameter is reduced from D_0 to D as the deformation proceeds (see *Figure 1a*).

In the simple shear tests, the polished and etched surface of the samples was engraved with a fine network of (originally) orthogonal markers, at a distance apart of 500 μm; from the distortions of these, the local shear γ is assessed according to the following equation:

$$\gamma = \tan(\theta) \quad (2)$$

where θ is the inclination angle of the transversal markers (*Figure 1b*).

RESULTS

Overall observation of the deformation processes

The micrographs in *Figure 4* show qualitatively the behaviour of individual spherulites at different stages

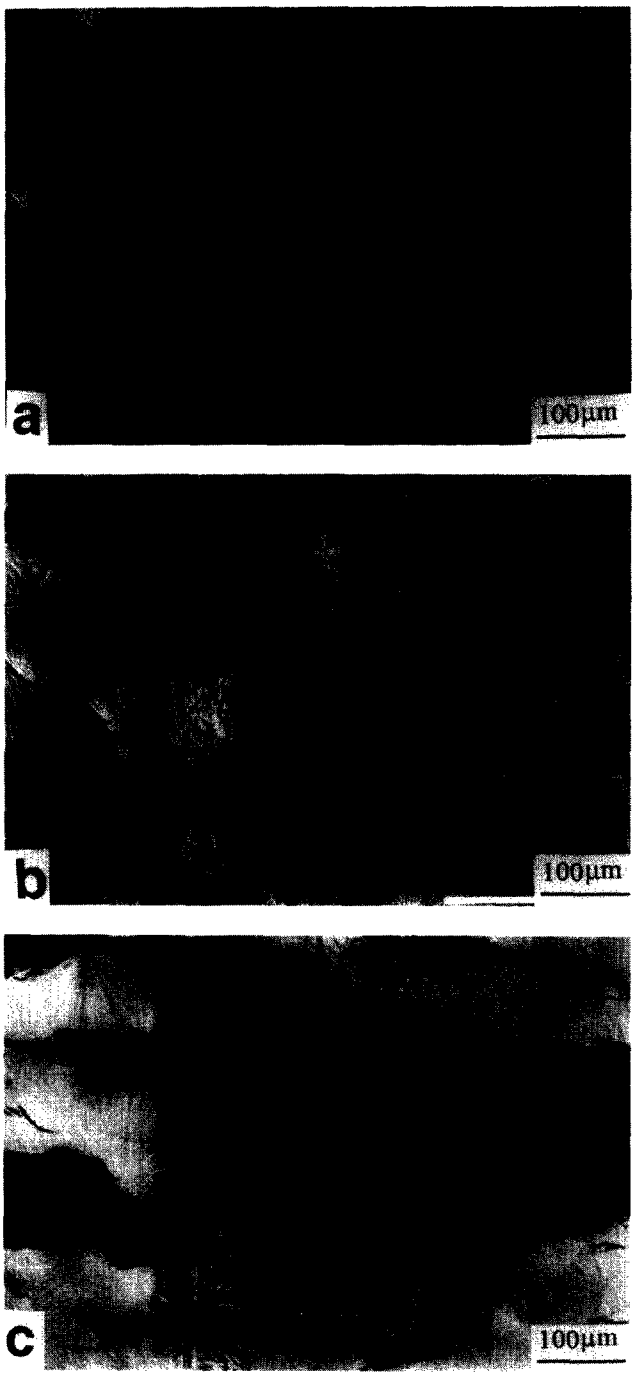

Figure 4 Evolution of the structure of PP during a uniaxial tensile test, where the bright central spherulites correspond to the β-phase: (a) $\varepsilon = 0$; (b) $\varepsilon = 0.1$; (c) $\varepsilon = 0.25$

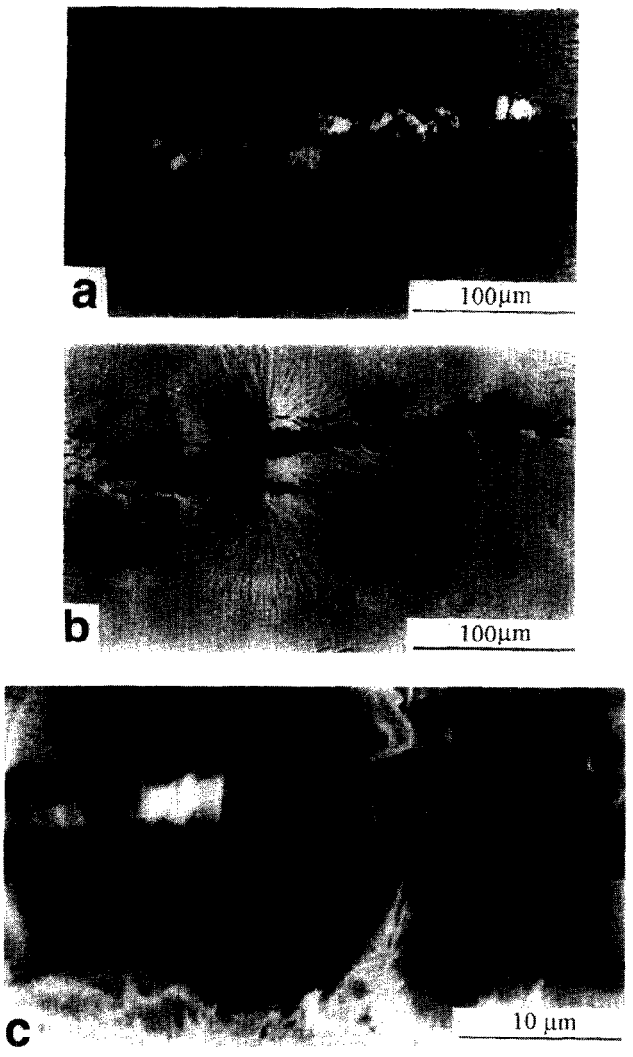

Figure 5 Complementary observations used to check that the crazing effects observed in *Figure 4* are actually intrinsic to the polypropylene material: (a) crazes observed during a tensile test; (b) the same zone after unloading and new gold sputtering; (c) an enlarged view of the microfibrils in a craze

during an experiment in uniaxial tension. In the reference micrograph of *Figure 4a*, obtained at rest, one may unambiguously differentiate the α- (dark) species at the periphery of the zone from the β- (bright) spherulites in the middle of the image. When the tensile test is carried out, it is clear that the α-phase exhibits the most brittle behaviour. Individual examination of the incipient crazes in this phase shows that they appear preferentially at the centre of the spherulites, grow parallel to a radial direction and eventually reorient their propagation direction perpendicularly to the tensile axis. This nucleation-and-growth geometry is clearly illustrated by the very contrasted craze which has appeared in the spherulite on the left-hand side of the micrographs. This craze originally grew along an oblique direction parallel to a set of radial lamellae (*Figure 4b*) and then turned to take up an horizontal path, ignoring the structural features of the underlying spherulites. Alternatively, in some cases (see, for example, the craze just above the preceding one) the flaws were nucleated at the spherulite boundary. In all cases, it is interesting to note that the propagation of the crazes finally leads to the formation of major cracks such as those which are dramatically visible in *Figure 4c*. In contrast to the preceding phenomena, the β- (bright) spherulites deform in a much more diffuse manner. The deformation process appears very early at the centre of the spherulites, and then propagates along an equatorial direction perpendicular to the tensile axis. The polar regions are attained only at a later period. It is not yet clear which contribution to this deformation process is taken up by shear banding and microcrazing mechanisms. Whatever the case, it is evident that the overall cohesion of these spherulites is preserved until very large strains are attained and that, in the case of *Figure 4c*, most of the residual tensile resistance of the material is supported by the β-phase alone.

It is important at this stage to cast off any doubt as to the reality of the crazing events observed in these tension experiments. The question as to whether the flaws that appear could be due to the artefactual breaking of the gold layer was ruled out by special tests in which the samples were deformed until the defects appeared (*Figure 5a*), unloaded, restained with gold and then put back into the scanning electron microscope for further analysis (*Figure 5b*). It can be seen from the latter micrograph that although the smaller crazes disappeared after this series of operations (merely as a consequence of the material relaxation), the major crazes remained unchanged. Furthermore, at a higher magnification (see *Figure 4c*), one can clearly see the fibrillar structure inside these flaws. It can therefore be stated that the features displayed by the SEM observations during these tests are representative of the actual evolution of the material.

When deformed under simple shear, the polypropylene spherulites do not show any extensive crazing, whatever their crystalline structure. As demonstrated in *Figure 6*, both phases are capable of bearing a very large shear deformation with no apparent damage, and they adopt a highly elongated shape, with the major axis along the principal strain axis of the simple shear distortion field. However, the deformation seems to be inhomogeneous. On a macroscopic scale, one can note that the horizontal and vertical markers become somewhat wavy, denoting shear strain fluctuations within the microstructure. Furthermore, when observing the individual spherulites in more detail, it appears that the β-spherulites adopt a higher contrast at their centres at large strains, while the α-species maintain a regular aspect. Although only qualitative, these points indicate that both phases behave in a different manner under load. The quanitative investigation of this non-homogeneity will be the subject of the next section.

Deformation analysis of individual spherulites

The plastic deformation of both phases was analysed in tension and in shear by means of a simple geometric method applied to individual spherulites. In this approach, the overall shear was compared with the local strain corresponding to the actual shape of selected spherulites observed in the micrographs obtained under load. The discrepancies between the overall and the spherulite deformations are then representative of the strain fluctuations among the spherulite population.

The case of uniaxial tension is illustrated in *Figure 7*. The micrographs show a selected zone at three successive stages of the test, with the true strain indicated for each stage being the overall deformation of the hourglass

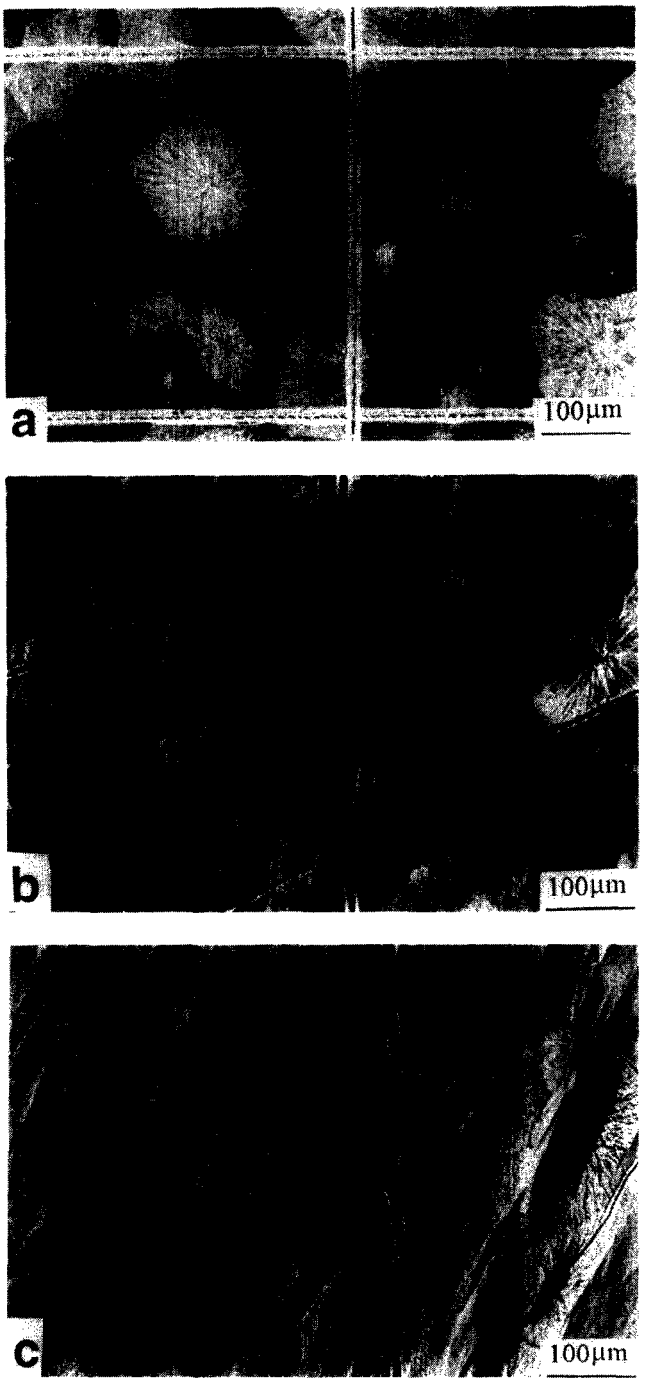

Figure 6 Evolution of the structure of PP during a simple shear test: (a) $\gamma = 0$; (b) $\gamma = 0.5$; (c) $\gamma = 1.5$

specimen within the central cross-section where the observed zone was located. The geometric shape corresponding to the initial configuration of *Figure 7a* was digitized from the contour of the central β-spherulite, while the other two shapes were computed from the initial contour by applying an extension ratio, $\lambda_z = \exp(\varepsilon_{sph})$, along the vertical tensile axis and a contraction ratio, $\lambda_r = \exp(-\varepsilon_{sph}/2)$, along the transverse axis, in order to obtain the best fit with the actual shape of the deformed spherulite. The parameter ε_{sph} introduced in this geometric transformation therefore measures the strain undergone by the spherulite under investigation. It is interesting to note that, while the spherulite strain remains nearly equal to the specimen strain for a small plastic deformation (*Figure 7b*), it becomes more than twice as large as the overall strain at large deformations (*Figure 7c*). By this time, the contribution of the α-spherulites to the deformation is less important and is mostly due to the development of cracks rather than to plastic processes.

The same type of analysis was also applied in the case of simple shear, with the spherulite shear γ_{sph} again being computed in order that that the theoretical contour matches the actual shape observed for the macroscopic shear γ applied to the sample. The geometric modelling presented in *Figure 8* shows that the local deformation of a selected β-spherulite exceeds, by $\sim 25\%$, the overall deformation of the sample at applied strains of 0.5 and 1.0. A correlation can be seen whereby the α-spherulites deform by about 25% less than the whole specimen (*Figure 9*). Here, the problem of heavy crazing decohesion is not encountered since both phases deform in a continuous way. With the volume fractions, f_α and f_β, of the α- and β-species, respectively, being almost equal to 50% in this material (according to a previous paper[4]), one can then estimate that the overall shear is given by a law-of-mixing of the type, $\gamma = f_\alpha \gamma_\alpha + f_\beta \gamma_\beta$, where γ_α and γ_β are the spherulitic strains, respectively, of the α- and β- phases.

Analysis of full-scale samples previously deformed with a standard testing machine

We have reported above the *in situ* analysis of α- and β-spherulites at the etched surface during the course of tension and shear tests performed with the miniaturized machine located inside the scanning electron microscope chamber. Although this methodology is very interesting, since it provides real-time information about the processes which control the deformation in each phase, one could question whether the observed features are really representative of what happens in the bulk during tests performed under normal conditions in a standard testing machine, or if the observations could be influenced by the following:

(i) the specific location at the surface of the deformed zone;
(ii) the previous etching of the microstructure;
(iii) the vacuum environment inside the scanning electron microscope;
(iv) the observations under load;
(v) the beam radiation.

In order to remove these doubts, specific experiments were performed in the following way: hourglass shaped specimens having double the dimensions of those used for the *in situ* experiments were deformed up to several levels of strain. The experiments were carried out on a tensile testing machine (MTS 810) at a strain rate of $5 \times 10^{-4}\ s^{-1}$. The deformation is measured through a video camera interfaced to a fast-processor microcomputer (Compaq 486, 66 MHz) which controls the servo-hydraulic actuator so that a constant deformation rate is maintained[13].

The tensile samples were deformed up to 0.4, unloaded, carefully truncated along the median plane and then polished carefully until no scratches were visible on the exposed surface. They were subsequently immersed in the etching solution, following the same procedure as

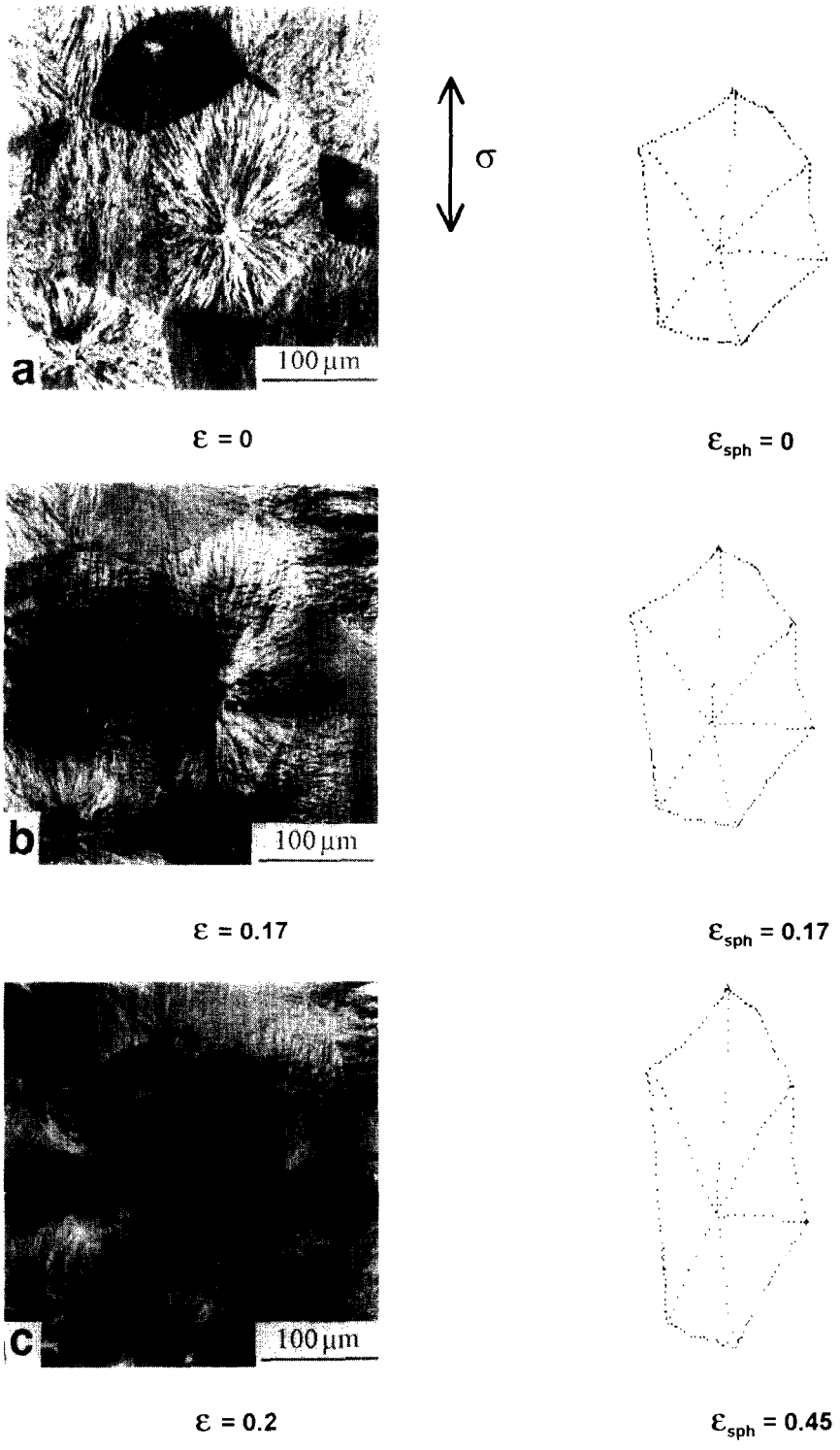

Figure 7 Modelling of the plastic behaviour of a β-spherulite of PP under tension. The shapes on the right are the theoretical contours which represent the best-fit with the actual shapes on the left by a uniaxial tension transformation from the original contour; the corresponding spherulite strain ε_{sph} is indicated on the figure

that described above and then finally stained to avoid excessive heating or electron deposition on the surface. The observations were performed in the scanning electron microscope.

The shear samples that were used also had double the dimensions of those used for the *in situ* observations. They were machined from the intruded plates in such a way that the observed surface coincides with the median plane of the plates (i.e. the plane where the β-spherulites are dominant). The specimens were deformed up to 1, unloaded, polished and then treated by the sulfochromic solution.

Under tensile loading (*Figure 10a*), the α-spherulites exhibit a brittle behaviour by propagation of cracks in the equatorial region and at the boundaries, perpendicular to the loading direction. In contrast, the β-spherulites exhibit a much more ductile behaviour. The evolution of spherulites of both phases is similar to that observed

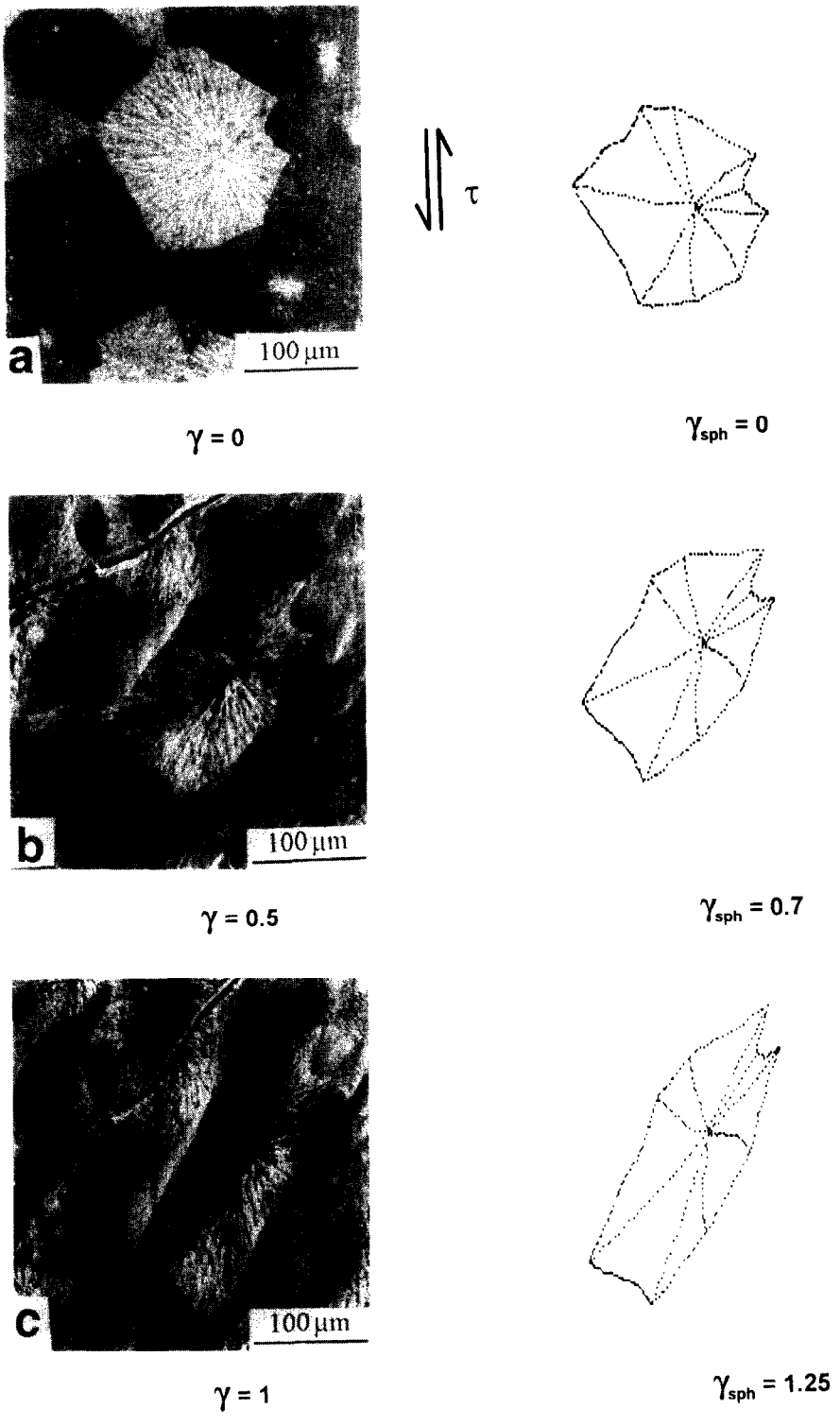

Figure 8 Modelling of the plastic behaviour of a β-spherulite of PP under shear. The theoretical shapes on the right correspond to the best fit with the actual shapes through a simple shear transformation γ_{sph}

during the tests performed *in situ* in the scanning electron microscope. However, since the etching is done after deformation, the acid solution diffuses faster through the cracks and crazes induced by the deformation. The etching is more aggressive and the cracks appear to be more widely opened than in the *in situ* observations. One should notice also that the electron micrographs obtained with the unloaded sample show less opened cracks compared with the *in situ* investigations. This is a consequence of the stress relaxation which takes place in the samples after they are unloaded.

In the shear experiment (*Figure 10b*) the α- and β-spherulites deform plastically up to high deformations without any observable damage in any of the two phases, as was also observed during the *in situ* experiments.

To summarize, it appears that the main features identified by *in situ* observations in the course of tensile and shear tests operated in the scanning electron

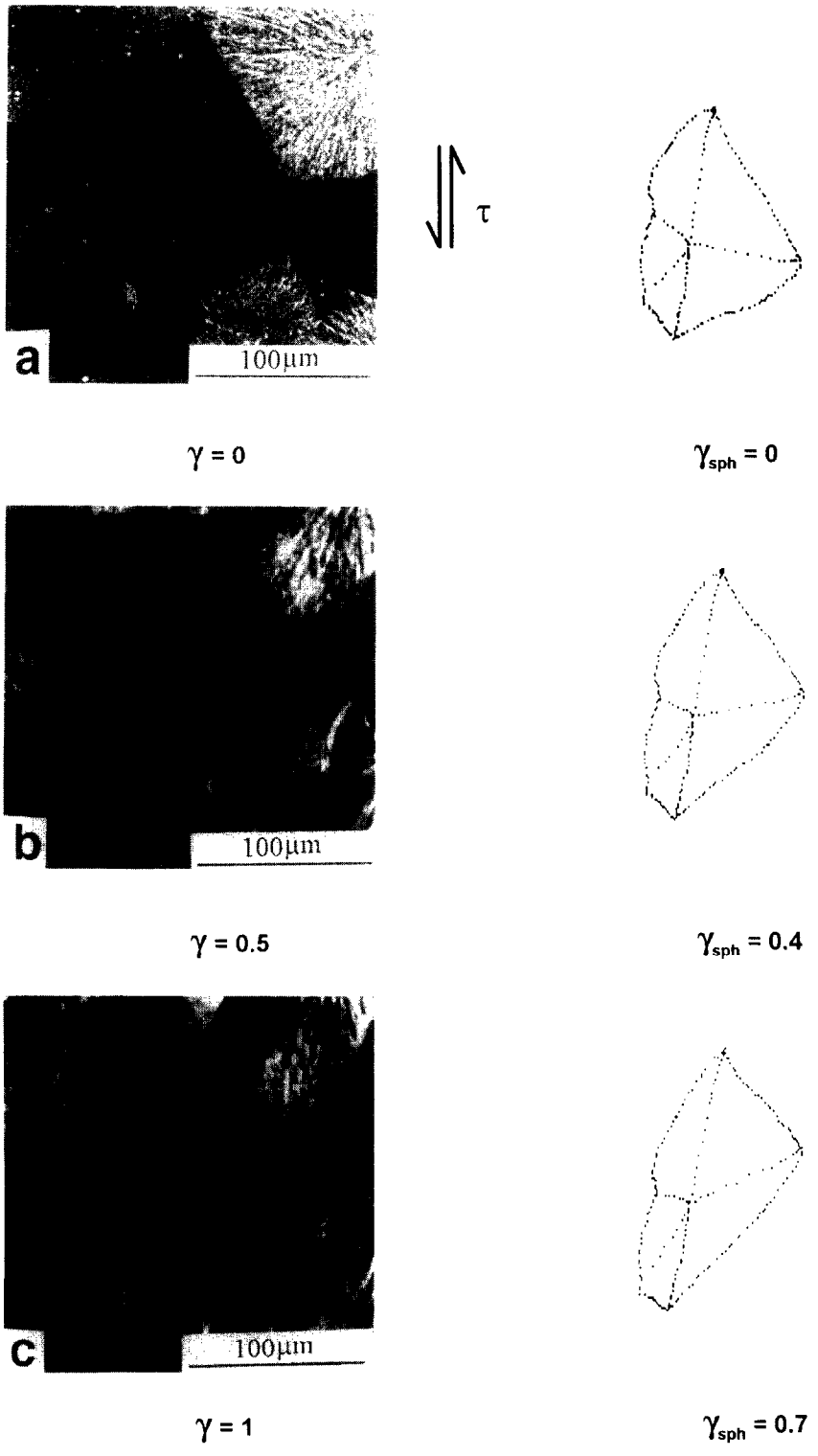

Figure 9 Modelling of the plastic behaviour of a α-spherulite of PP under shear. The theoretical shapes on the right correspond to the best fit with the actual shapes through a simple shear transformation γ_{sph}

microscope chamber are found again when the microscope observations are performed with specimens deformed prior to the chemical etching. Although the particular conditions of the mechanical tests run inside the microscope chamber can possibly induce some perturbations to the deformation process, the observations reported here indicate that these perturbations are not detectable, if they exist at all, with respect to the major mechanisms identified for the α- and β-spherulites.

DISCUSSION

The experimental results reported in the previous section show that the large-spherulite polypropylene samples investigated here exhibit deformation mechanisms which are typical of the crystalline structure and of the loading mode. In this section the attention will be focused on the micromechanical aspect of the observed phenomena in relation to the structural features of the α- and β-phases.

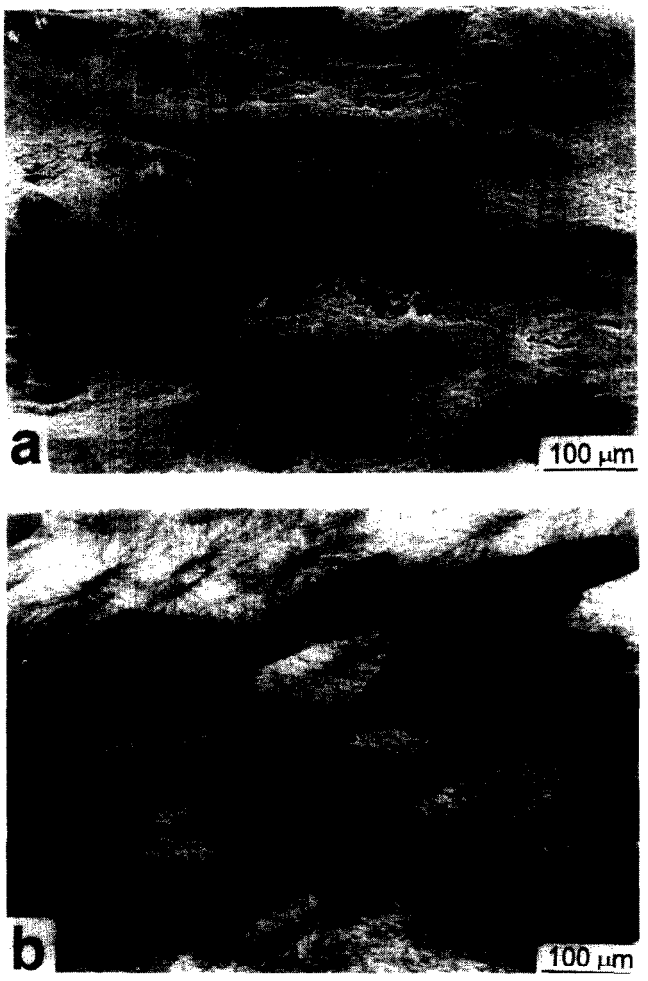

Figure 10 The behaviour of α- and β-spherulites in PP samples previously deformed outside the scanning electron microscope chamber, and subsequently revealed by etching: (a) in tensile mode ($\varepsilon = 0.4$); (b) in shear mode ($\gamma = 1.0$)

Structural bases

It is now well established, after the early pioneering works[2-4], that the structural complications of polypropylene arise not only from the two allotropic forms encountered in this material (monoclinic for the α-phase *versus* hexagonal for the β-phase), but also from the different growth morphologies of the crystalline lamellae. Surprisingly enough, the β-phase (which is the less developed one in most industrial samples has the simplest morphological features, since the hexagonal lamellae grow radially with either more or less curvature or twisting (*Figure 11a*), somewhat like that seen in the reference case of polyethylene. The thickness of the crystalline lamellae is of the order of only 10 nm, with the chain direction (*c*-axis) oriented perpendicular to the major faces of the crystals. This means that the macromolecules do not fit simply into the thickness of material available but are presumably folded back and forth several times, unless they are engaged within several adjacent crystallites through tie molecules. The lamellae grow radially from nucleation points in the form of spherulites, with the *b*-direction along the radial line. In contrast to the above case, the monoclinic lamellae in the α-phase are of two types[14] (*Figure 11b*). In the first case, the primary crystallites grow along the spherulite radius; they have a ribbon-like shape and their growing direction coincides with their a^*-direction (projection of the *a*-vector along the direction perpendicular to the *bc*-plane). The secondary set of crystallites grows along the tangential direction of the spherulites in the interstices between the primary lamellae. There is some kind of epitaxy between the two sets of crystals, with the *c*- and a^*-directions of the radial lamellae matching the a^*- and *c*-axes of the tangential crystals, respectively. In both phases, a certain fraction of the macromolecular chains remains entrapped in an amorphus structure between the crystallites. These are constituted, for their major part, of tie molecules joining two adjacent lamellae or by loose folds of chains re-entering the same lamella.

The deformation of semicrystalline structures, such as those encountered in the PP under investigation here, is controlled by several basic mechanisms. Since the van der Waals bonds between the non-adjacent organic groups are much weaker than the covalent bonds along the chains, the former contribute more to the apparent elastic compliance of the crystals. Consequently, the in-plane modulus of the crystalline lamellae is three orders of magnitude more than the modulus of the amorphous zones since, as the glass transition temperature is low ($T_g \approx -20$°C), the interlamellar chains are in a rubber-like state at room temperature. At large strains, the deformation of the semicrystalline polymers is essentially controlled by plastic slip mechanisms with crystalline dislocations moving on a selection of glide planes along prescribed directions[15,16]. Since in all crystalline forms of PP the polymeric chains are oriented in the direction of the *c*-axis, perpendicular to the lamellae, dislocations will appear only in planes containing the *c*-axis because the energy needed for dislocations to distort the covalent bonds would be excessive. As for the critical resolved shear stress (CRSS) which is necessary to activate the formation and glide of

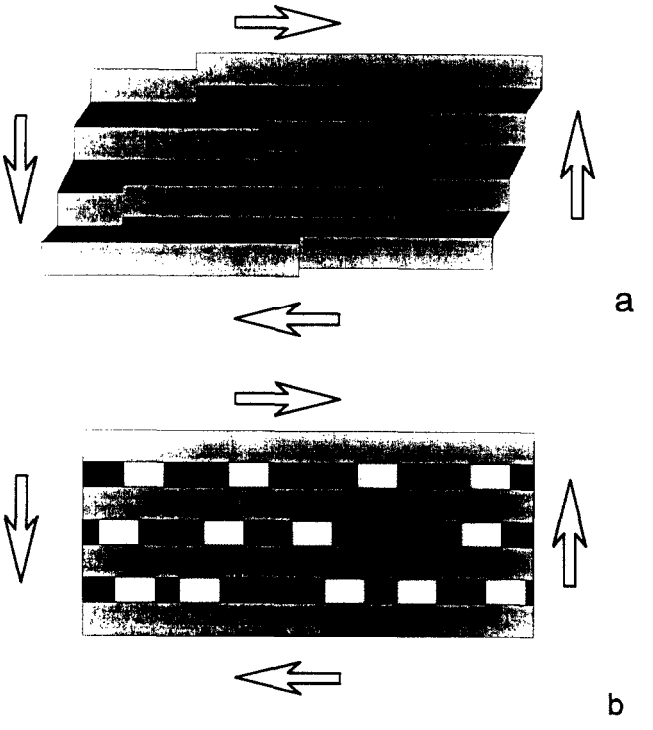

Figure 11 Schematic structures of the lamellae in polypropylene: (a) radial curved lamellae in the β-phase; (b) radial and tangential lamellae in the α-phase

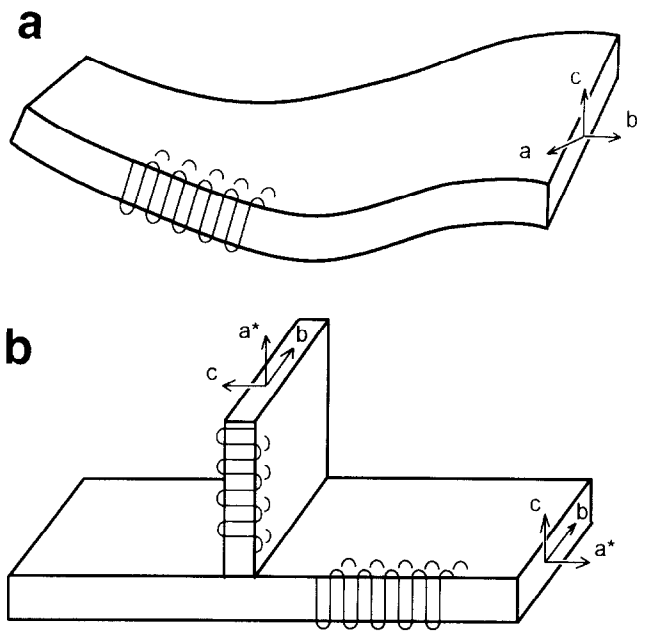

Figure 12 Schematic representation of the microscopic response of a stack of PP lamellae in a generalized shear field: (a) random glide, accommodated by the amorphous phase in the β-phase; (b) interlocking effect of the tangential crystallites in the α-phase

dislocations, this is still the subject of debate because it is not accessible directly from simple experiments. It is obvious that in most cases, the CRSS is lower for the 'chain-slip' systems (whose glide direction is along the c-axis) than for the 'transverse slip' systems, whose activation requires the displacement of crystalline block perpendicular to the chains, along a very rough glide plane. In the monoclinic α-structure, the easiest glide system is (010) $\langle 001 \rangle$. The other systems can be ordered according to an increasing CRSS: (100) $\langle 001 \rangle$, (110) $\langle 001 \rangle$, $(1\bar{1}0)$ $\langle 001 \rangle$, and (010) $\langle 100 \rangle$. As for the hexagonal β-phase, very little information is available on its plastic behaviour; nevertheless it can be deduced from the symmetry of the lattice that the CRSS should increase in the following order: $\{10\bar{1}0\}$ $\langle 0001 \rangle$, $\{10\bar{1}0\}$ $\langle \bar{1}210 \rangle$. Therefore not only is the interpretation of experimental results on the plastic deformation in PP complicated because of the lack of reliable data concerning the glide systems, but in addition to this, the fine morphology of the lamellae in both phases (curved radial ribbons in the β-phase versus tangential crystallites interlocked with the radial lamellae in the α-phase) plays a considerable role.

As is illustrated schematically in *Figure 12*, the application of a generalized shear field has different effects in the two cases. In the β-phase (*Figure 12a*), with the crystalline lamellae only being linked by the rubber-like chains, the elementary shear can be accommodated by the neighbouring amorphous material and no correlation is needed between the plastic events occurring in the adjacent lamellae. Consequently, the creation and movement of the dislocations can occur at any place and the crystal glide is easy. In comparison, the activation of plastic glide requires much more correlation in the α-phase. As illustrated schematically in *Figure 12b*, the tangential crystals imbricated in the radial lamellae act as 'keys' in the crystalline architecture; shearing a given lamellae must be accommodated by the deformation of other crystallites. Let us consider, for example, a glide process initiated in a radial lamella along the (010) $\langle 001 \rangle$ glide system, which requires the lowest energy (chain slip in the c-direction). The propagation of this process into a daughter tangential lamella requires the continuity of the shear plane and direction. From the geometric sketch of *Figure 11b*, the glide in the daughter crystallite should propagate in the transverse glide system (010) $\langle 100 \rangle$, which is more difficult. The situation is even worse if the shear is nucleated along the second easy system, i.e. (100) $\langle 001 \rangle$, of the radial lamellae since it should continue on the (001) $\langle 100 \rangle$ glide system, which unrealistically cuts the chain axis. Consequently, unless complicated cross-slip mechanisms are involved, the propagation of glide across successive radial and tangential crystallites seems difficult and it is more likely that plastic deformation would act only by propagation of the shear in the free 'channels' of amorphous chains between the tangential lamellae. It is easy to imagine that the percolation of such shearing paths is not very favourable and that damage should soon appear in the α-spherulites.

Spherulite deformation under uniaxial tension

The systematic observation of the contrast changes within individual β-spherulites under tension (such as those displayed in *Figure 4*) indicates that the first deformation events occur near the centre, as noted previously in polybutene films stretched in a special tensile stage in a polarizing microscope[17,18]. These results are not unexpected, since the theoretical calculations of Wang[19] (although based on linear elasticity assumptions) show that this central region of the spherulites is subjected to a significant stress concentration. Also, the latter analysis shows that the equatorial region of the spherulites undergoes a high tensile stress component which is likely to stretch preferentially the amorphous tie molecules joining the radial crystalline lamellae which are perpendicular to the tensile axis (*Figure 13a*). The lamellar separation is presumably the cause of the marked contrast effects observed in the corresponding region of the β-spherulites under tension at moderate strains (see *Figure 4b*). In the polar region, the spherulites seem to undergo very little deformation. This is because in this region the lamellae are oriented with their b-axis parallel to the loading direction (*Figure 13c*), in such a way that the crystallites (whose elastic modulus is higher than 3000 MPa) act as a reinforcing platelets among the rubber-like matrix and that the resolved shear stress on the plastic glide systems is particularly low. Furthermore, in this region the transversal compression strain tends to pack the chains in the amorphous phase, thus increasing the interrelation beween the lamellae. Finally, it is in the regions which are oriented at ± 45 with respect to the loading direction that the β-lamellae are subjected to the highest shear strain along the active glide systems, since they are radially oriented. This shearing strain also contributes to the tilt of the lamellae and brings them towards the orientation which is perpendicular to the loading direction. Eventually, at higher elongations, the plastic deformation of the spherulites induces the breaking of the lamellae and creates a fibrillar structure. This ultimate evolution starts from the equatorial region and proceeds towards the polar part of the spherulites[20].

In contrast, the α-spherulites exhibit no appreciable

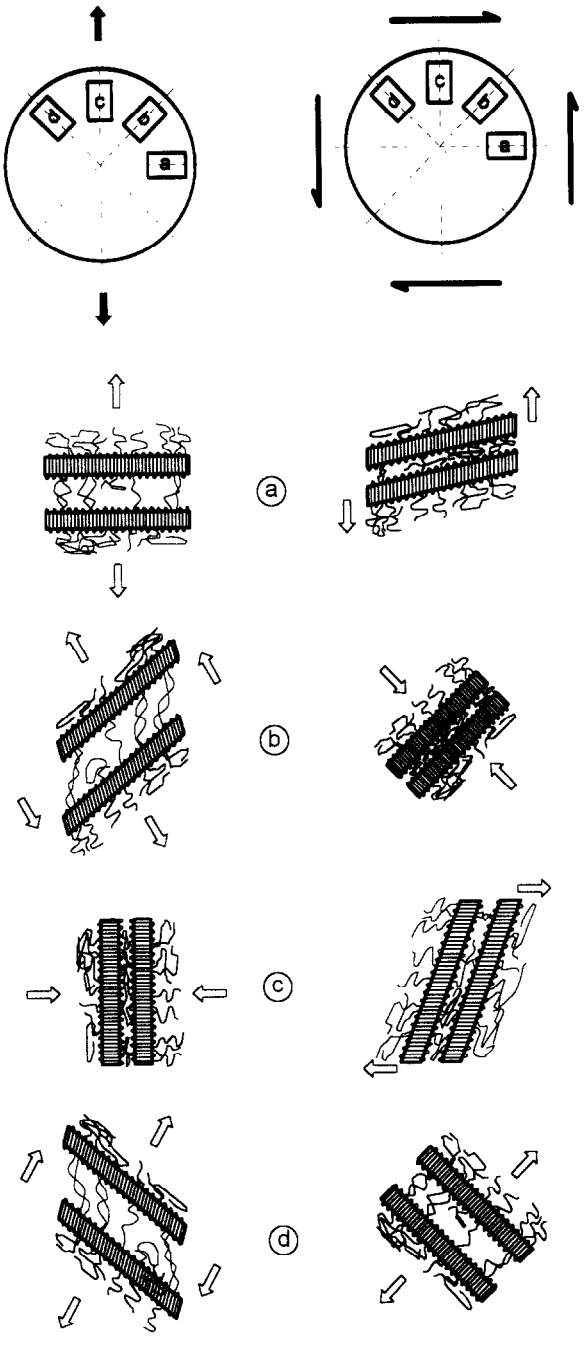

Figure 13 Behaviour of the different sectors in PP spherulites under uniaxial tension and simple shear: the black arrows represent the applied stresses and the open arrows the locally active deformation modes

deformation in the early stages of tensile testing, while the β-spherulites begin to exhibit a dark band in their equatorial region. This behaviour for the α-phase results from the interlocking effect of the radial lamellae by the tangential crystallites that we have described above. The presence of the daughter crystallites in the interstitial regions beween the radial lamellae makes the deformation of the amorphous chains much more difficult and, furthermore, limits the lamellar separation in the equatorial region of the spherulites. In addition, the plastic slip acting in the regions oriented at $\pm 45^{\circ}$C with respect to the loading direction is considerably hindered by the interlocking structure of the α-spherulites (*Figure 12*). The continuation of the plastic deformation requires a higher energy because lamellar tilting in this region requires the in-block rotation of neighbouring lamellae connected by the tangential crystals.

Another interesting point concerning the α-spherulites is the occurrence of cracks along the boundaries between the spherulites. Wittkamp and Friedrich[21] and Jang *et al.*[22] had previously noticed this phenomenon in specimens with spherulites as large as ours. It seems that this effect could be due in part to the high compliance of the boundaries and also to the concentration of defects (low-molecular-weight chains, impurities, etc.) which preferentially accumulate in these zones during the growth of the spherulites. Therefore, in the particular case of a coarse spherulitic structure, the boundary zones must accommodate high stress concentrations and develop crazing and cracking preferentially under the highly dilatant strain field of the tensile test.

Finally, the feasibilty of large tensile deformations in PP depends on what will prevail in the competition between plastic shear mechanisms and craze damaging for the accommodation of the applied stretch. While in the present test at room temperature only the β-phase is capable of exensive plasticity, a recent study[23] has shown that purely α-phase samples (obtained by annealing for 1 h at 155 C) could be deformed plastically in tension up to $\varepsilon \sim 1.5$, providing that the test is run at 70 C. One can deduce that at this temperature shear bands take over the plastic deformation as opposed to the cavitation mechanisms.

Shear deformation

Our experiments with the shear apparatus used in this work have shown that both the α- and β-spherulites can reach very high strains in this deformation mode which do not subject the material to important hydrostatic stresses. A brief discussion, similar to the one concerning the tension measurements, will help in understanding what happens within the sheared spherulites.

Similar to the case of uniaxial tension, the behaviour of individual crystallites depends upon their location within the spherulites, but now the principal axes of stress (tension and compression) are oriented along directions oblique to the shear direction. The angle of inclination is ± 45 in the initial stage of the shear tests, and subsequently the principal extension direction rotates toward the macroscopic shear direction. In a given spherulite the zones which favour the plastic glide in the radial lamellae are those where the chains are inclined at 0 and 90 with respect to the shear direction (*Figure 13*, zones a and c). As we have observed in another publication[24], the combination of plastic slip systems in these zones provokes a gradual rotation of the chains in such a way that a marked crystalline texture is formed in which the chain axis is parallel to the shear direction. Conversely, in the oblique zones (*Figure 13*, zones b and d) the radial direction coincides either with tension or compression stresses, in such a way that, as a first step, only the amorphous phase is subjected to extensive deformation. The effect of this deformation is noticeable in the micrographs of *Figures 6b* and *6c* by the development of dark lines radially oriented in the β-spherulites, in particular in the zones where the amorphous chains are subjected to extension. In the α-phase, it can be seen that the spherulites deform

qualitatively in the same way as in the β-phase. The important damaging effects observed in tension are no longer encountered here because the dilatant hydrostatic effects are now negligible. However it was noted in *Figures 8* and 9 that the α-spherulites deform less than the β-spherulites because of the interlocking effect of the tangential lamellae.

CONCLUSIONS

Polypropylene samples were subjected to tensile and shear tests after their surfaces had been polished and etched in order to reveal the substructure characterized by large spherulites. The *in situ* observation of the structural features under load reveals specific evolutions of the α- and β-spherulites up to large strains.

In the tensile experiments, the two crystalline modifications behave very differently. The β-spherulites undergo deformation at small strains. The process begins in the centre of the spherulites, propagates in the equatorial region, and then progressively invades the zones inclined at ± 45 with respect to the loading direction. This evolution seems to involve several basic mechanisms, including lamellar separation, crystalline plastic slip and eventually crazing. The α-spherulites appear to maintain an elastic response for a longer time as the macroscopic stretch is applied but then suddenly exhibit intensive crazing which leads to the formation of cracks propagating either in the middle of the spherulites (originally along a radial direction) or at the boundaries between the spherulites.

Under simple shear, both phases are capable of undergoing very high shear deformations. No early crazing is observed, due to the absence of any hydrostatic stress. Nevertheless, there is still a difference in the behaviour of both phases. The α-phase deforms less than the β-phase, with the average shear of the specimen being intermediate. A form of composite law-of-mixing could thus be ascribed to this dual-phase material.

The difference in the α- and β-spherulite behaviours was related to their contrasting structures. The β-spherulites contain only radial lamellae of a hexagonal structure which are more or less curved, while the α-phase is typically composed of radial and tangential lamellae of a monoclinic structure. This interlocked structure stiffens the latter spherulites and makes the plastic glide of the α-phase very difficult, so that the damaging mechanisms predominantly control the overall response.

ACKNOWLEDGEMENTS

The authors are indebted to Drs B. Echalier and J. M. Muracciole, of the Atochem company (Cerdato, Serquigny, France) for kindly providing the material and also for valuable discussions.

REFERENCES

1 Natta, G., Corradini, P. and Cesari, M. *C. Rend. Acad. Naz. Lincei.* 1956, **21**, 365
2 Khoury, F. *J. Res. Natl. Bur. Stand.* 1966, **A70**, 29
3 Padden, F. J. and Keith, H. D. *J. Appl. Phys.* 1959, **30**, 1479
4 Norton, D. R. and Keller, A. *Polymer* 1985, **26**, 704
5 Aboulfaraj, M., Ulrich, B., Dahoun, A. and G'Sell, C. *Polymer* 1993, **34**, 4817
6 G'Sell, C. and Jonas, J. J. *J. Mater. Sci.* 1979, **14**, 583
7 Boni, S., G'Sell, C., Weynant, E. and Haudin, J. M. *Polym. Test.* 1982, **3**, 3
8 G'Sell, C., Jacques, D. and Favre, J. P. *J. Mater. Sci.* 1989, **24**, 2004
9 Olley, R. H. and Basset, D. C. *Polymer* 1982, **23**, 1707
10 Basset, D. C. and Olley, R. H. *Polymer* 1984, **25**, 935
11 Olley, R. H. and Bassett, D. C. *Polymer* 1989, **30**, 399
12 G'Sell, C. *Rev. Phys. Appl.* 1988, **23**, 1085
13 G'Sell, C., Hiver, J. M., Dahoun, A. and Souahi, A. *J. Mater. Sci.* 1992, **27**, 5031
14 Lotz, B. and Wittmann, J. C. *J. Polym. Sci., Polym. Phys. Edn.* 1986, **24**, 1541
15 Balta-Calleja, F. J. and Peterlin, A. *J. Macromol. Sci.-Phys.* 1970, **4**, 519
16 Young, R. J. and Bowden, P. B. *J. Mater. Sci.* 1974, **9**, 2034
17 Weynant, E., Haudin, J. M. and G'Sell, C. *J. Mater. Sci.* 1980, **15**, 2677
18 Weynant, E., Haudin, J. M. and G'Sell, C. *J. Mater. Sci.* 1982, **17**, 1017
19 Wang, T. T. *J. Polym. Sci. Polym. Phys. Edn.* 1974, **12**, 145
20 Schultz, J. 'Polymer Materials Science', Prentice-Hall, Englewood Cliffs, NJ, 1974, p. 466
21 Wittkamp, I. and Friedrich, K. *Prakt. Metallogr.* 1978, **15**, 321
22 Jang, B. Z., Uhlmann, D. R. and van der Sande, J. B. *Polym. Eng. Sci.* 1985, **25**, 28
23 Dahoun, A. *PhD Thesis* Ecole des Mines de Nancy, France, 1992
24 Dahoun, A., G'Sell, C., Canova, G. R., Philippe, M. J. and Molinari, A. in 'Textures and Microstructures' (Ed. H. J. Bunge), Vols 14–18, Gordon and Breach, London, 1991, p. 347